Energy Impact of Ventilation and Air Infiltration
14th AIVC Conference, Copenhagen, Denmark
21-23 September 1993

Modelling Adjustable Speed Drive Fans to Predict Energy Savings in VAV Systems

D Lorenzetti

Building Technology Group,
M.I.T. Department of Architecture, Room 4-209,
77 Massachusetts Avenue, Cambridge, MA 02139, USA

Modeling Adjustable Speed Drive Fans to Predict Energy Savings in VAV Systems

David M. Lorenzetti
Department of Architecture
Massachusetts Institute of Technology
Cambridge, Massachusetts

SYNOPSIS

The momentum balance on a centrifugal fan, supplemented by a complete energy balance for rigorous interpretation of power-pressure interactions, relates these variables to flow rate and fan speed. Nonideal behavior is modeled by direct mechanical interpretation and by engineering correlation, leading to more general expressions than provided by the fan laws. First attempts to fit these expressions to measured data show promise but reveal limitations of current practice in the data collection and reporting process.

LIST OF SYMBOLS

Variables

a	Arbitrary pressure coefficient
A	Effective flow area
b	Arbitrary power coefficient
c	Absolute velocity of air [=] m/s
d	Characteristic fan size [=] m
e	Reynolds variation exponent [=] 1
f	Moody friction factor [=] 1
$\dot{m}$	Mass flow rate [=] kg/s
n	Fan speed [=] rpm
p	Pressure [=] $kg/m{\cdot}s^2$
P	Power [=] $kg{\cdot}m^2/s^3$
r	Radial distance [=] m
Re	Reynolds number [=] 1
T	Torque [=] $kg{\cdot}m^2/s^2$
u	Impeller linear velocity [=] m/s
$\bar{u}$	Specific internal energy [=] m^2/s^2
w	Air velocity relative to impeller [=] m/s
α	Kinetic energy factor [=] 1
β	Velocity diagram angle
ε	Absolute surface roughness [=] m
ϕ	Flow coefficient [=] 1
η	Efficiency [=] 1
μ	Dynamic viscosity [=] kg/m·s
ρ	Density [=] kg/m^3
ω	Angular velocity [=] s^{-1}
ψ	Head coefficient [=] 1

Operators, subscripts, and overscripts

{ }	Functional relationship
[=]	Has the units of
1	Of fan, at entrance to impeller
2	Of fan, at exit from impeller
exit	At fan exit
eye	At fan entrance
fan	Through or across fan
fan	Of power, delivered by fan to air
idl	Ideal result for lossless case
imp	Through or across impeller
θ	Tangential component
r	Radial component
shft	Of power, required at drive shaft
z	Axial component
$\bar{}$	Vector quantity
*	At zero slip

1. INTRODUCTION

In a Variable Air Volume (VAV) ventilation system, a central fan supplies a variable flow rate of air to the conditioned spaces. Flow is regulated by dampers, inlet vanes, or by speed modulation of the fan, to meet the temperature and fresh air requirements of the local zones served by the fan. A return fan, similarly regulated, exhausts air from the zones.

Dampers and inlet vanes govern flow by increasing losses of mechanical energy along the flow path, thus decreasing the flow rate through the duct. If the same, lower, flow rate is established by decreasing fan speed, mechanical energy losses are reduced in the fan, rather

than increased in the duct. Thus fan speed control is preferred from a power standpoint [1]. Field measurements have shown 45 to 65% energy savings for adjustable-speed drive (ASD) retrofits of inlet vanes on VAV supply fans [8], and a related study showed 20 to 45% additional savings if the system controller is redesigned to take advantage of the fan's new range of pressure-flow characteristics [9].

To estimate savings in existing ventilation systems, and to predict the performance of novel system control strategies, requires a model of the fan's pressure, flow, and power characteristics at different speeds. Currently, polynomial curves are fit to data measured at a single speed, and adjustable-speed operation is accounted for using the "fan laws"-- scaling factors based on similarity arguments between the variables of interest. This paper applies mass, momentum, and energy conservation principles to a centrifugal fan, using correlations from engineering practice to account for deviations from ideal behavior. The resulting model is matched to performance data and the results discussed in light of the fan laws.

2. FAN LAWS AND DIMENSIONLESS CURVE FITS

The fan laws are based on a dimensional analysis of the flow variables, together with the assumptions that: (1) the flow regime remains fully turbulent in all passages, so that Reynolds number effects on friction are negligible; and (2) wall roughness effects scale approximately with pump size [11]. The flow variables-- pressure rise Δp, mass flow rate $\dot{m}$, fan size d, fan speed n, air density ρ, air viscosity μ, and surface roughness ε-- may be nondimensionalized in terms of [11]: (1) the head coefficient $\psi = \Delta p/(\rho n^2 d^2)$; (2) the flow coefficient $\phi = \dot{m}/(\rho n d^3)$; (3) the Reynolds number based on the linear speed n·d of the impeller $Re_{nd} = (\rho n d^2)/\mu$; and (4) relative roughness ε/d. Neglecting the last two terms by the assumptions above,

$$\psi = \frac{\Delta p}{\rho n^2 d^2} \approx \psi\left\{\frac{\dot{m}}{\rho n d^3}\right\} = \psi\{\phi\} \qquad (1)$$

If two fans from the same geometric family operate at $\phi_2 = \phi_1$, then by Equation 1, $\psi_2 = \psi_1$. These give the familiar fan law for geometrically similar fans [1]:

$$\text{for } \dot{m}_2 = \dot{m}_1 \frac{\rho_2}{\rho_1}\frac{n_2}{n_1}\left(\frac{d_2}{d_1}\right)^3 \text{ then } \Delta p_2 = \Delta p_1 \frac{\rho_2}{\rho_1}\left(\frac{n_2}{n_1}\right)^2\left(\frac{d_2}{d_1}\right)^2 \qquad (2)$$

Setting power $P = \dot{m}(\Delta p/\rho)$, a second fan law, $P_2 = P_1 \cdot (\rho_2/\rho_1) \cdot (n_2/n_1)^3 \cdot (d_2/d_1)^5$, follows.

Typically $\psi\{\phi\}$ in Equation 1 is approximated as $\psi = a_0 + a_1\phi + a_2\phi^2 + a_3\phi^3 + a_4\phi^4$, where coefficients a_i are to be determined by fits to measured data [2]. Substituting,

$$\Delta p = a_0\rho\omega^2 + a_1\dot{m}\omega + a_2\frac{\dot{m}^2}{\rho} + a_3\frac{\dot{m}^3}{\rho^2\omega} + a_4\frac{\dot{m}^4}{\rho^3\omega^2} \qquad (3)$$

For convenience, fan size d, and the factor converting from n to ω, have been absorbed in the coefficients a_i. By expressing ψ as a function of ϕ only, Equation 3 implicitly satisfies the fan law as it would be applied to a single fan ($d_2 = d_1$) in order to estimate how a change in density or fan speed would affect mass flow and pressure rise.

A polynomial expression for power as a function of flow can be defined in the same way-- the dimensionless power coefficient is $P/(\rho n^3 d^5)$ [11]. A second method is to: (1) write the power delivered to the air as $P_{fan} = \dot{m}(\Delta p/\rho)$; and (2) express efficiency $\eta = b_0 + b_1\phi + b_2\phi^2 + b_3\phi^3 + b_4\phi^4$ so that shaft power $P_{shft} = P_{fan}/\eta$ is the ratio of two polynomials in $\dot{m}$, ρ, and ω [2]. Strictly Δp should be the "total" pressure rise, that is, the sum of the pressure form of all mechanical energy rises. However for curve-fitting purposes this probably is not necessary, as the change of kinetic energy usually is small and the coefficients b_i need not be physically interpretable.

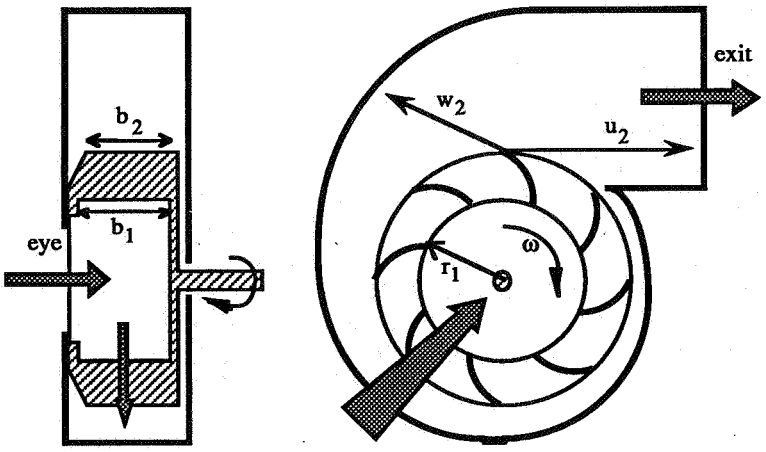

Figure 1. A centrifugal fan with backward-tipped impeller blades.

3. PHYSICAL LAW, ENGINEERING CORRELATION, AND THE FAN

In the classical treatment of centrifugal machines (see e.g. [3, 11]), a momentum balance, applied to an idealized, lossless impeller, yields an expression for fan power which is then: (1) combined with terms accounting for friction and shear forces to give shaft power; and (2) recast into an impeller pressure-rise relation. Finally, empirical relations are used to account for mechanical energy losses in the fan. This last step, of modifying the ideal pressure rise expression, has been described mainly by researchers seeking to predict the behavior of a centrifugal machine in its design stages [3, 10, 12] or to improve estimations of the pressure-flow relation at low flow conditions [4, 7].

3.1. Definitions

Figure 1 shows a centrifugal fan with backward-inclined blades, for which air, exiting the impeller with relative velocity $\overline{w_2}$, has a tangential speed $w_{\theta 2}$ acting in the opposite direction from the linear speed $\overline{u_2}$ of the blade tips. With forward-tipped blades, $\overline{w_2}$ is in the same direction as $\overline{u_2}$; however, no impeller guides air perfectly, and $w_{\theta 2}$ always is smaller than if air came off exactly at the angle of the blade [3], a phenomenon known as slip.

Figure 2, a velocity diagram for the impeller exit, shows the effect of slip as air exits at an angle $\beta_2 < \beta_2^*$, the blade angle. Air leaves the impeller with absolute velocity $\overline{c_2} = \overline{u_2} + \overline{w_2}$, the vector sum of the blade tip speed and the air velocity relative to the tip. Figure 2 also shows the tangential and radial components, $c_{\theta 2}$ and c_{r2}, of the absolute velocity. Numerous estimates of slip, summarized in [5, 10], have been made; most yield an expression of the form $\cot(\beta_2) = \cot(\beta_2^*) + (\text{constant})\cdot(u_2/c_{r2})$, which is used henceforward.

A similar velocity diagram may be drawn at the inner impeller radius. Slip at the impeller entrance is treated by assuming that either: (1) $\overline{c_1}$ is always radial [3], so that $c_{\theta 1} = 0$ and β_1 varies with flow; or (2) β_1 remains constant, usually at the blade angle β_1^* [5, 10].

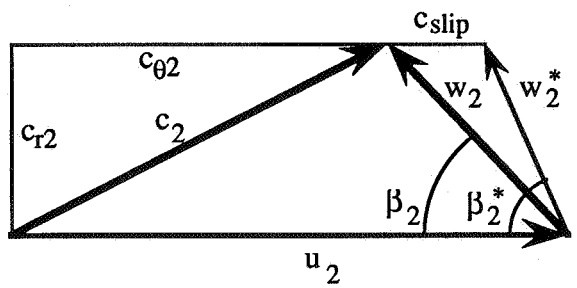

Figure 2. Velocity diagram at the impeller exit.

3.2 Momentum Conservation in the Lossless Impeller

The application of momentum conservation to a lossless centrifugal impeller is treated in detail in e.g. [3, 11]; the following overview highlights the idealizations made. At steady-state, conservation of angular momentum requires the sum of applied moments to balance the net rate of outflow of angular momentum from the control volume [11]. For the annular region between the impeller entrance and exit, the moments include the torque T transmitted through the shaft, and those due to bearing friction and shear forces from the flow of air along the blades. These last two are neglected for the idealized, lossless, process, but are included later. Since pressure forces act radially they produce no moment. Taking ω positive as shown in Figure 1, torque acts in the positive axial direction and therefore only the axial component of angular momentum leaving the control volume need be considered.

Only the tangential component of the fluid velocity produces an axial moment, so the outward angular momentum flux is $\int(r_2 c_{\theta 2})d\dot{m}$ at the impeller exit and $\int(-r_1 c_{\theta 1})d\dot{m}$ at its inlet, where the flow is into the control volume. Combining, the momentum balance gives torque $T = \dot{m}_{imp}(r_2 c_{\theta 2} - r_1 c_{\theta 1})$ for the lossless impeller.

Fan power is $P = \omega T$, and using $u = \omega r$,

$$P_{idl} = \dot{m}_{imp}(u_2 c_{\theta 2} - u_1 c_{\theta 1}) \qquad (4)$$

From the velocity diagram, $c_{r2}\cot(\beta_2) = u_2 - c_{\theta 2}$. The slip expression described above gives $\cot(\beta_2)$, and for incompressible flow the radial velocity is given by $\dot{m}_{imp} = \rho A_2 c_{r2}$. Estimates of the reduction of flow area A_2 from its maximum of $2\pi r_2 b_2$, taking into account blade thickness and recirculation effects at the periphery of the impeller [3, 10], show no dependence on mass flow or angular velocity. Therefore A_2 is treated as constant, although separation effects, which influence A_2, play a role in impeller efficiency [12]. Since A_2 already incorporates scaling factors, it is not necessary to assume c_{r2} is uniform over the flow area; only that the velocity profile across each blade passage remains similar, regardless of flow rate.

The inlet geometry is similar, although slip is treated differently, as mentioned above. The question of slip at the impeller inlet can be rendered moot by extending the control volume into the impeller core so that air crosses the control surface in the axial, rather than the radial, direction. In this case the momentum flux at the inlet becomes $\int(-r \cdot c_{\theta eye})d\dot{m}$, integrated from $r = 0$ to r_1. The tangential velocity at the inlet, $c_{\theta eye}$, sometimes known as "swirl" [12], accounts for the power benefit associated with inlet vanes over dampers [1]: while both regulate flow through dissipation, inlet vanes impart a prerotation to the air.

However slip is treated at the impeller entrance, the ideal power relation reduces to

$$P_{idl} = b_1 \dot{m}_{imp}\omega^2 + b_2 \frac{\dot{m}_{imp}^2 \omega}{\rho} \qquad (5)$$

where constants b_1 and b_2 incorporate the physical and experimental parameters.

3.3 Nonideal processes affecting fan power

The ideal power expression must be modified to include the nonideal processes affecting fan power. These are: (1) bearing loss due to friction in the shaft bearings, for which power is proportional to ω [3, 10]; and (2) disc loss, the power needed to overcome friction torque on the impeller surfaces [3, 5, 10]. From $P = \omega T$, disc power is proportional to ω times a shear force; note that this treatment of disc power departs from that of [3, 5, 10], which use $P = \Delta p \cdot A \cdot v$ rather than $P = \omega T$.

The shear forces influencing disc loss, derived by analogy with turbulent duct flow, are proportional to ρv^2 [11]. The characteristic velocity is ω in the core and on external surfaces, and w_2 in the blade passages. The disc friction power terms are: (1) $\rho\omega^3$ in the core; and (2) $\dot{m}_{imp}\omega^2$, $\dot{m}_{imp}^2\omega/\rho$, and $\rho\omega^3$ in the flow passages, after $w_2^2 = c_{r2}^2(1 + \cot^2\beta_2)$ is substituted from the velocity diagram. Then shaft power becomes

Source of power term	$\dot{m}\omega^2$	$\frac{\dot{m}^2\omega}{\rho}$	$\rho\omega^3$	ω
Ideal power	√	√		
Disc power in core			√	
Disc power in core, Reynolds variation			$\frac{\surd}{\rho^e\omega^e}$	
Disc power in flow passages	√	√	√	
Disc power in flow passages, Reynolds variation	$\frac{\surd}{\dot{m}^e}$	$\frac{\surd}{\dot{m}^e}$	$\frac{\surd}{\dot{m}^e}$	
Bearing power				√

Table 1. Summary of shaft power terms and their sources. Power terms with Reynolds variation are divided by the appropriate Reynolds relation as shown.

$$P_{shft} = b_1\dot{m}_{imp}\omega^2 + b_2\frac{\dot{m}_{imp}^2\omega}{\rho} + b_3\rho\omega^3 + b_4\omega \qquad (6)$$

where the b_i in Equations 5 and 6 are not related.

Frictional losses sometimes are assumed to vary with Reynolds number as $(Re)^{-e}$ where $0.2 \le e \le 0.25$ [5, 10]. Reynolds number is related to $\rho\omega$ in the impeller core, and to $\dot{m}_{imp}$ in the blade passages. Table 1 summarizes, by analytic source, the candidate terms for a shaft power expression, and the effect on them of assuming friction varies with Re.

Among the nonideal processes not counted are: (1) variations in velocity profile or effective flow area; (2) impeller losses, described below, which transform pressure work into internal energy within the control volume; and (3) any processes taking place outside the control volume, which transform the energy already contained in the air stream.

3.4 Pressure rise in the impeller

In the conventional development, the ideal power expression of Equation 4 is compared with a power equation in the total pressure [3, 11], followed by geometrical substitutions [3] to show the total pressure rise is the sum of: (1) a dynamic rise $(\rho/2)\cdot(c_2^2 - c_1^2)$; (2) a static rise $(\rho/2)\cdot(u_2^2 - u_1^2)$ due to centrifugal forces of rotation; and (3) a static rise $(\rho/2)\cdot(w_1^2 - w_2^2)$ due to decreasing velocity in the widening flow channel [3, 4]. The same result can be found by integrating Newton's second law along a streamline, considering centrifugal and pressure forces but neglecting shear [3, 4]. Both approaches ignore the complete energy equation-- the first by substituting for power from a partial energy balance, and the second by avoiding power altogether. In either analysis, the power terms must be considered to arise because of pressure drops, when in fact they contribute, albeit inefficiently, to pressure rise.

For incompressible adiabatic flow at steady-state, conservation of energy in the impeller may be expressed [11]

$$\frac{p_2 - p_1}{\rho} = \frac{P_{fan}}{\dot{m}_{imp}} + (\tilde{u}_1 - \tilde{u}_2) + \frac{1}{2}(\alpha_1 c_1^2 - \alpha_2 c_2^2) \qquad (7)$$

where: (1) P_{fan}, the net rate at which energy is added to the air stream, includes shear work at the control surfaces; (2) $\tilde{u}$ is the internal energy per unit mass of air; and (3) α, the kinetic energy correction factor, accounts for the fact that in a stream moving with average speed c, the average kinetic energy per unit mass is not $c^2/2$.

P_{fan} is given by e.g. Equation 6, excepting the bearing loss power $b_4\omega$, which the motor provides to the shaft but which is not transmitted to the fluid. Disc power is transmitted to the fluid though not primarily as a pressure rise. Perhaps 30% of disc power is returned as useful work [5], recovered as pressure in the volute [10]. This suggests that the immediate effect of disc friction is to increase the kinetic energy of the flow.

Finally, $\tilde{u}_2$ increases as mechanical energy is lost through viscous and turbulent dissipation. Engineering practice is to express such hydraulic losses as either [10]:

(1) dynamic (mixing and shock) losses of the form $\Delta p \propto \rho v^2$; or (2) friction losses of the form $\Delta p \propto f \rho v^2$, where friction factor f may vary with Reynolds number.

Impeller dynamic losses include: (1) entry shock due to the equivalent of slip at the impeller inlet, modeled as a mismatch velocity akin to c_{slip} in Figure 2 [3, 5, 10]; (2) profile drag on the impeller blades, modeled as a relative speed w [10]; and (3) wake shedding from the blades at the impeller exit, modeled as a sudden expansion loss in c_{r2} [10].

Impeller friction losses are attributed to a representative relative velocity w [3, 5, 10]. Where disc power treats friction as a force producing a torque, impeller friction treats friction as a mechanism transforming the input power from pressure work to internal energy. Therefore the terms generated by these hydraulic losses are not quite the same as those due to disc friction. Table 2 demonstrates the differences between the terms.

3.5 Nonideal processes in the fan entrance and volute

Energy balances similar to Equation 7 may be written from the eye to the impeller inlet, and from the impeller outlet to the fan exit. Summing the three equations yields an expression for the fan pressure rise. Replacing changes in internal energy by the engineering approximations of the hydraulic loss terms,

$$p_{exit} - p_{eye} = \rho \frac{P_{fan}}{\dot{m}_{imp}} + \frac{1}{2}\rho(\alpha_{eye}c_{eye}^2 - \alpha_{exit}c_{exit}^2) + \rho g(z_{eye} - z_{exit}) - \Sigma\Delta p_{loss} \quad (8)$$

where the pressures and kinetic energies internal to the fan have canceled, and the possibility of changes in gravitational potential energy has been admitted.

Due to leakage between the high- and low-pressure sides of the fan, the mass flow through the impeller will be higher than that through the fan. Leakage flow $(\dot{m}_{imp} - \dot{m}_{fan}) \propto \sqrt{\rho \Delta p_{imp}}$ [10]; unfortunately this expression leads to an implicit equation in $(p_2 - p_1)$. Thus this nonideality is ignored, and henceforward, $\dot{m}_{imp} = \dot{m}_{fan}$.

Velocities c_{eye} and c_{exit} are related to mass flow by the density and the inlet and exit areas; the contribution of these terms, with α taken as constant, is given in Table 2. Note that at low flows the assumption α_{exit} constant is especially problematic due to recirculation in the discharge duct [1, 7]. Hydraulic losses in the eye and volute are summarized in [3, 5, 10] and produce the same functional terms as in the impeller; see Table 2.

Source of pressure term	$\rho\omega^2$	$\dot{m}\omega$	$\frac{\dot{m}^2}{\rho}$	$\frac{\rho^2\omega^3}{\dot{m}}$	ρ
Ideal power	√	√			
Disc power in core				√	
Disc power in core, Reynolds variation				$\frac{\sqrt{}}{\rho^e\omega^e}$	
Disc power in flow passages	√	√		√	
Disc power in flow passages, Reynolds variation	$\frac{\sqrt{}}{\dot{m}^e}$	$\frac{\sqrt{}}{\dot{m}^e}$		$\frac{\sqrt{}}{\dot{m}^e}$	
Impeller dynamic losses	√	√	√		
Impeller friction losses	√	√	√		
Impeller friction losses, Reynolds variation	$\frac{\sqrt{}}{\dot{m}^e}$	$\frac{\sqrt{}}{\dot{m}^e}$	$\frac{\sqrt{}}{\dot{m}^e}$		
Entrance hydraulic losses	√	√	√		
Volute hydraulic losses	√	√	√		
Change in kinetic energy			√		
Change in potential energy					√

Table 2. Summary of pressure terms and their sources.

Pressure model	Sum of squares [=] in^2		
	12" fan	20" fan	44" fan
Δp = average	5935	2627	574
$\Delta p = a_0n^2 + a_1n{\cdot}Q + a_2Q^2$	1.6	0.93	5.4
$\Delta p = a_0n^2 + a_1n{\cdot}Q + a_2Q^2 + a_3n^3/Q$	0.18	0.27	0.73

Table 3. Error sums of squares for data fits to the simplest fan law pressure models.

4. MODEL TERMS AND THE FAN LAWS

Compared to the analytic pressure terms, the polynomial $\psi\{\phi\}$ in Equation 3: (1) contains two dimensionally correct but physically uninterpretable terms, ϕ^3 and ϕ^4; (2) does not contain the term $\rho^2\omega^3/\dot{m}$, corresponding to ϕ^{-1}; (3) does not contain a term ρ; and (4) does not account for variations of friction with Re. The first two differences relate to the choice of $\psi\{\phi\}$, while the last two relate to the assumptions made in writing $\psi = \psi\{\phi\}$, i.e., no dependence on gravity or Reynolds number. Similarly, a dimensionless power function would not be able to incorporate Reynolds variation or the dependence of power on ω, though the other analytic terms would be given by ϕ^0, ϕ, and ϕ^2.

The model terms were fit using three sets of data: (1) 441 records for a 12", single-inlet fan, taken from a manufacturer's data table; (2) 487 data records, read from a second manufacturer's table for a 20", double-inlet fan; and (3) 92 records, read from the first manufacturer's fan curve for a 44", single-inlet machine. Each record consisted of n [=] rpm, volume flow Q [=] cfm, Δp [=] in. w.g., and P [=] hp. Because density was not varied in the data tables, Q was substituted for $\dot{m}$ and ρ was dropped from each of the model terms, assumed to be absorbed in the model coefficients; likewise, n was substituted for ω.

The terms were fit by least-squares estimation. Partial results for the pressure fits are shown in Table 3. For example, in the 12" fan, using a model $\Delta p = a_0n^2 + a_1n{\cdot}Q + a_2Q^2$ reduces a sum of squares about the mean of 5935 in^2 to an error sum of squares of 1.6 in^2. The reduction of the sum of squares using a four-term model, by factors on the order of 10^4 for the tabular data, and of 10^3 for data interpolated from a fan curve, suggests that the data presented by the manufacturers received some prior conditioning, either by application of the fan laws or by analytic treatment such as that described above.

In fact the data reported by a fan manufacturer typically has undergone two trend-weakening manipulations: (1) pressure-flow points recorded at a fixed fan speed are interpolated by cubic spline fits; and (2) the fan laws are applied to extrapolate the interpolated points to different fan speeds and fan sizes [6]. Applying the fan laws conditions the data, tending to strengthen the apparent contribution of terms derived from the fan laws, and to weaken those terms which do not conform to the fan law assumptions, e.g. those showing the empirical variation of friction with Reynolds number. Still it is possible to detect the effect of Reynolds number variation in the data.

The following numerical experiment demonstrates this conditioning of the data: (1) 20 pressure points were generated using $\Delta p = nQ^{0.75}$ with n = 100 rpm and Q increasing from 5 cfm by steps of 5 cfm; (2) the 20 points were extrapolated by the fan law to new curves at n = 10, 20, 50, and 150 rpm; (3) the resulting 100 points were fit by least-squares estimation, using both the generating formula $\Delta p = a_0nQ^{0.75}$, and the relation $\Delta p = a_0n^2 + a_1n{\cdot}Q$; and (4) it was observed that the error sum of squares from the fan law estimate was lower, by a factor of 0.6, than that due to the original formula. Thus a five-fold multiplication of the data weakens their defining relationship to the point where a two-term fan law can be judged superior. Since the tabular data are reported at varying rpm, the conditioning effect of applying the fan laws extends to virtually every point in a manufacturers' reported fan data-- not just to 80% of them.

It is possible, by algebraic evaluation, to rewrite the functional form of each term in Table 2 to account for the effect of applying the fan laws. If density is held constant, the end result is to multiply each term with Reynolds variation by ω^e. Fitting the new terms to the

data gives an order of magnitude improvement in the error sums of squares, an effect which would not be expected if there was in fact no variation of friction with Reynolds number. However, it is impossible using this method to distinguish Reynolds effects due to changes in ω, since the original data were measured at a single speed.

5. CONCLUSION

Analytic expressions have been developed for power and pressure in a centrifugal fan. These may be expected to represent fan behavior more accurately than do the fan laws, and preliminary data fits show evidence of the nonideal behavior modeled. However if the data to be fit are extrapolated from single-speed measurements using the fan laws, there is little incentive to seek more general or rigorous formulations. In any fan model, the choice of terms can be guided by physical law as well as by functional convenience.

ACKNOWLEDGEMENTS

This work is the outgrowth of a research project financially supported by EUA Cogenex, Northeast Utilities, and the Empire State Energy Research Corporation. The author also wishes to acknowledge the contributions and continued support of J.W. Axley and L.K. Norford, both of the Massachusetts Institute of Technology.

REFERENCES

1. ASHRAE, 1988. *1988 ASHRAE Handbook, Equipment*, SI Edition. American Society of Heating, Refrigerating and Air-Conditioning Engineers, Inc., Atlanta.

2. Brandemuehl, M.J. et al, 1992. "A Toolkit for Secondary HVAC System Energy Calculations." American Society of Heating, Refrigerating and Air Conditioning Engineers, Inc., Atlanta.

3. Eck, B.E., 1973. *Fans; the design and operation of centrifugal, axial-flow, and cross-flow fans*. Translated by Azad, R.S. and Scott, D.R. Pergamon Press, Oxford.

4. Engeda, A. and Rautenberg, M., 1989. "On the Flow in a Centrifugal Pump Near Shut-Off Head with Positive and Negative Flows," Eleventh International Conference of the British Pump Manufacturer's Association, April 1989, pp. 1-7. Springer-Verlag, Berlin.

5. Dick, E. and Belkacemi, M., 1992. "Optimum Design of Centrifugal Fans and Pumps," European Journal of Mechanical Engineering, v. 37, no. 1, March 1992, pp. 9-18.

6. Franklin, M. Personal communication. Twin City Fan and Blower, Minneapolis.

7. Frost, T.H. and Nilsen, E., 1991. "Shut-off Head of Centrifugal Pumps and Fans," Proceedings of the Institution of Mechanical Engineers, Part A: Journal of Power and Energy, v. 205, no. A3, pp. 217-23.

8. Lorenzetti, D.M. and L.K. Norford, 1992. "Measured Energy Consumption of Variable-Air-Volume Fans Under Inlet Vane and Variable-Speed-Drive Control," ASHRAE Transactions, Vol. 98, Part 2, 1992, pp. 371-79.

9. Lorenzetti, D.M. and L.K. Norford, 1993. "Pressure Reset Control of Variable Air Volume Ventilation Systems," Proceedings of the ASME International Solar Energy Conference, April 1993, pp. 445-53. American Society of Mechanical Engineers, New York.

10. Neumann, B., 1991. *The Interaction Between Geometry and Performance of a Centrifugal Pump*. Mechanical Engineering Publications Ltd., London.

11. White, F.M., 1979. *Fluid Mechanics*. McGraw-Hill Inc., New York.

12. Wilson, D.G., 1989. *The Design of High-Efficiency Turbomachinery and Gas Turbines*, 4th printing. The MIT Press, Cambridge, Massachusetts.